ON THE NUMERICAL RECONSTRUCTION OF THE THREE-DIMENSIONAL DENSITY OF THE MEDIUM IN THE ACOUSTIC SYSTEM OF EQUATIONS

D. V. KLYUCHINSKIY
N. S. NOVIKOV
M. A. SHISHLENIN

Представлено С.И. Кабанихиным

Abstract: In the article it is considered a gradient method for solving a 3D coefficient inverse problem of determining the density of a medium for a hyperbolic acoustic system using a finite number of measurements. The inverse problem is reduced to minimizing the cost functional by the gradient method. A numerical algorithm for solving the coefficient inverse problem is implemented and the gradient of the residual functional is obtained by solving the corresponding conjugate problem. Within the framework of a model experiment simulating ultrasound tomography of human tissues, the results of restoring the three-dimensional density coefficient of the medium are presented.

Keywords: 3D ultrasound tomography, gradient method, optimization, 3D coefficient inverse problem, hyperbolic acoustics system, Godunov method.

1   Introduction

In this work we consider and implement numerical algorithms for solving a three-dimensional coefficient inverse problem of ultrasound tomography of human soft tissues. The development of methods and algorithms for solving problems that allow the use of ultrasound sensing for the diagnosis of malignant neoplasms in human soft tissues at an early stage has been actively conducted recently [14, 16, 19, 25, 24, 26, 27, 28]. Such problems are formulated in the form of inverse problems in which it is necessary to find the parameters of a mathematical model based on measurement additional data at the boundary of the domain [54].

The characteristic features of inverse problems are both their ill-posedness and the large amount of computing resources needed to obtain an approximate inverse problem solution. Therefore, the development of algorithms that make the most effective use of available additional information is very important.

Of the many mathematical models that can be used to solve ultrasound tomography problems, models based on a second-order equation or on a hyperbolic system of first-order equations are most often considered [30, 31, 34]. Models based on second-order equations [17, 21, 23, 51] are more theoretically investigated. However, the assumptions necessary for the application of second-order equations often do not allow us to guarantee the reliability of solving the direct, and therefore the inverse problem from a physical point of view [23]. The approach proposed in this paper is based on the use of a system of first-order acoustic equations as the main process model and, although it is more resource-intensive from the point of view of a numerical solution, it has the advantage that the close connection of the system of equations with conservation laws causes the proximity of the numerical solution to real wave processes in the object under study, and also allows you to model diagrams the directionality of acoustic wave sources [38]. For the first time, a two-dimensional inverse problem for a hyperbolic system of first-order equations for determining the two-dimensional density of a medium was numerically investigated in [18], the inverse problem was reduced to minimizing the target functional by gradient descent and the gradient of the functional was obtained through solving the corresponding conjugate problem, the Godunov scheme was applied to solve the direct and conjugate problems. Further, in the work [22], a two-dimensional coefficient inverse problem for a hyperbolic system for determining the wave propagation velocity and density was also investigated. The inverse problem was reduced to minimizing the Tikhonov functional with a TV-regularizing additive and a gradient of the functional was obtained.

Note that coefficient inverse problems for hyperbolic systems were theoretically investigated in [4]. Numerical methods for solving inverse problems were considered in the works [4, 31, 34].

The uniqueness and stability of coefficient inverse problems for hyperbolic equations with data given on a cylindrical boundary were in [10, 11, 53].

For the linear equation of acoustics, the ray formulation of the inverse problem of determining three unknown variable coefficients in the equation based on data measured at the boundary of the region where sources and receivers located was investigated [44]. It was proved that such an assignment of additional information allows us to uniquely find all three desired coefficients. Algorithmically, the original problem splits into three sequentially solved problems: the inverse kinematic problem of determining the speed of sound and two problems of integral geometry on a family of geodesic lines determined by the speed of sound.

A comparative analysis of five imaging and inversion methods was carried out: time-of-flight tomography, the method of focusing with a synthesized aperture, migration in reverse time, inversion in the Born approximation and inversion of the contrast source [49] on synthetic data representing a two-dimensional scan of a breast cancer tumor.

A three-dimensional computational model of the sensor [40] has been developed, which allows use the reconstruction methods based on the 3D waveform inversion in ultrasound tomography.

The inverse problem of recovering two coefficients in an acoustic equation by internal measurement data [52] was investigated. Using Carleman estimates it was proved the Lipschitz stability estimates and uniqueness of the inverse problem solution.

The inverse tomographic wave problem of recovering the characteristics of a diffuser in the form of spatial distributions of sound velocity, medium density, absorption coefficient and power index of its frequency dependence, as well as the flow velocity vector was investigated [35].

A numerical solution of the acoustic tomography problem was presented using an iterative and functional analytical algorithm based on the approach of R. Novikov [39].

The numerical method for restoring acoustic attenuation in a hyperbolic system of acoustic equations was presented [60]. It was shown that the recovery method was unstable.

It should also be mentioned that recently there have been many works based on the application of machine learning technologies in ultrasound tomography [42, 41, 45].

Nonlinear effects of ultrasound tomography have been investigated in the works [55, 56, 20, 33, 43].

It should be noted that 3D formulations of ultrasound tomography problems and numerical methods for their solution were considered, for example, in [20, 21, 29, 48, 40, 47].

Since we use a mathematical model based on a system of acoustic equations, in the course of solving the corresponding inverse problem, it is necessary to recover all parameters of the model, which are the density of the medium and the velocity of wave propagation. However, algorithms for finding several

coefficients in partial differential equations with a finite number of observations are even more time-consuming and have a number of features that must be taken into account during the numerical solution of [?]. Therefore, in this article, as a first step in the study of the three-dimensional inverse problem, we consider the problem of determining only the density of the medium.

2   Direct problem

Formulation.   Let us consider the following direct problem of acoustic wave propagation in a three-dimensional medium in the region
$\Omega = \{(x, y, z) : x \in (0, L), y \in (0, L), z \in (0, L)\}$, $t \in (0, T)$:

$$\frac{\partial u}{\partial t} + \frac{1}{\rho}\frac{\partial p}{\partial x} = 0, \quad \frac{\partial v}{\partial t} + \frac{1}{\rho}\frac{\partial p}{\partial y} = 0, \quad \frac{\partial w}{\partial t} + \frac{1}{\rho}\frac{\partial p}{\partial z} = 0, \tag{1}$$

$$\frac{\partial p}{\partial t} + \rho c^2 \left(\frac{\partial u}{\partial x} + \frac{\partial v}{\partial y} + \frac{\partial w}{\partial z} \right) = \theta_\Omega(x, y, z)I(t). \tag{2}$$

Equations (1)—(2) are obtained from the laws of conservation of momentum in the directions x, y and z, the law of conservation of mass. To finalize the problem formulation, we add the initial conditions

$$u, v, w, p|_{t=0} = 0 \tag{3}$$

and non-reflective boundary conditions. Functions $u = u(x, y, z, t)$, $v = v(x, y, z, t)$, $w = w(x, y, z, t)$ — components of the velocity vector in variables x, y and z respectively, $p = p(x, y, z, t)$ — function of the exceeding (acoustic) pressure, $\rho = \rho(x, y, z)$ — density of the medium, $c = c(x, y, z)$ — the velocity of wave propagation in the medium. Since the values of acoustic models are close to the values of the speed of sound and density of liquid media, we use the (1)—(3) system, which often occurs when describing the propagation of ultrasonic waves in liquid media. The function $\theta_\Omega(x, y, z)$ on the right hand side of the equation (2) is a characteristic function of the source in terms of spatial location, the time form of the source $I(t)$ has the following form (Riker pulse with dominant frequency ν_0) [22, 23]:

$$I(t) = \sin\left(\pi\nu_0(t - \frac{1}{\nu_0})\right) e^{-\pi\nu_0\left(t - \frac{1}{\nu_0}\right)}. \tag{4}$$

Well-posedness of the direct problems for linear hyperbolic systems were investigated in [15].

Method for solving a direct problem.   Here we provide a brief description of the method used to numerically solve a direct problem in the numerical experiments. The method is based on a counterflow scheme developed by S.K. Godunov.

This approach is based on the use of the integral form of the problem in combination with piecewise constant approximation of state variables inside numerical cells, as well as solving the Riemann problem.

To describe the method of numerical solution of the problem (1)—(3), consider a generalization of the equations (1)—(2) in the following form:

$$\frac{\partial \mathbf{U}}{\partial t} + \frac{\partial \mathbf{F}(\mathbf{U})}{\partial x} + \frac{\partial \mathbf{G}(\mathbf{U})}{\partial y} + \frac{\partial \mathbf{H}(\mathbf{U})}{\partial z} = 0. \tag{5}$$

Here $\mathbf{U} = (u, v, w, p)$ is a vector of state variables, and the functions $\mathbf{F}(\mathbf{U})$, $\mathbf{G}(\mathbf{U})$, $\mathbf{H}(\mathbf{U})$ respectively, the functions of the stream. After discretization we obtain the following relations:

$$\mathbf{U}^{i-1/2,j-1/2,k-1/2} = \mathbf{U}_{i-1/2,j-1/2,k-1/2} -$$
$$- \frac{\tau}{h_x} \left(\mathbf{F}_{i,j-1/2,k-1/2} - \mathbf{F}_{i-1,j-1/2,k-1/2} \right) -$$
$$- \frac{\tau}{h_y} \left(\mathbf{G}_{i-1/2,j,k-1/2} - \mathbf{G}_{i-1/2,j-1,k-1/2} \right) -$$
$$- \frac{\tau}{h_z} \left(\mathbf{H}_{i-1/2,j-1/2,k} - \mathbf{H}_{i-1/2,j-1/2,k-1} \right). \tag{6}$$

The equation (6) corresponds to the cell $(i - 1/2, j - 1/2, k - 1/2)$, where the subscript denotes the values of the state variables $\mathbf{U}$ at the current time step, and the superscript - respectively at the next time step. h_x, h_y, h_z, τ — grid steps in spatial and time coordinates, respectively. The values of the flows $\mathbf{F}$, $\mathbf{G}$, $\mathbf{H}$ are considered at the cell boundary, and are solutions to the Riemann problem (the problem of the decay of the gap) [50]. For example, the approximation (6) of the first of the equations (1) has the following form:

$$\rho u^{i-1/2,j-1/2,k-1/2} = \rho u_{i-1/2,j-1/2,k-1/2} +$$
$$+ \frac{\tau}{h_x}(P_{i,j-1/2,k-1/2} - P_{i-1,j-1/2,k-1/2}). \tag{7}$$

Considering the fact that the value $p = P_{i,j-1/2,k-1/2}$ is a solution to the problem of the decay of the gap posed at the boundary $\{i, j - 1/2, k - 1/2\}$ of the cell in question, we obtain the following relation:

$$p = \frac{p_{i-1/2,j-1/2,k-1/2} + p_{i+1/2,j-1/2,k-1/2}}{2} -$$
$$- \rho_0 c_0 \frac{u_{i+1/2,j-1/2,k-1/2} - u_{i-1/2,j-1/2,k-1/2}}{2} \tag{8}$$

The formula for calculating the velocity at the boundary $u = U_{i,j-1/2,k-1/2}$, which is part of the approximation of the fourth equation in (1), takes the following form:

$$u = \frac{u_{i-1/2,j-1/2,k-1/2} + u_{i+1/2,j-1/2,k-1/2}}{2} -$$
$$- \frac{p_{i+1/2,j-1/2,k-1/2} + p_{i-1/2,j-1/2,k-1/2}}{2\rho_0 c_0} \tag{9}$$

The other three equations of the (1) system are considered in a similar way. Adding the right hand side of the equations to the numerical solution scheme

is carried out in the same way. We do not give the all formulas that make up the numerical scheme. These relations, as well as the study of the stability of the scheme, are given, for example, in [50].

3   The inverse problem of density recovering

As part of the formulation of the direct problem (1)—(3) we assumed that the system parameters (density and velocity of sound in the medium) are known. However, in many applications it is necessary to solve the inverse problem and determine the parameters of the medium from additional measurements. Let us assume that additional information is obtained by measuring the acoustic pressure inside a certain number of receivers:

$$p(x, y, z, t) = f_k(x, y, z, t), \qquad (x, y, z) \in \Omega_k, \quad k = 1, \dots, N. \qquad (10)$$

This condition corresponds to a system of N receivers located in the corresponding area of Ω_k. We suppose that the speed of sound in the medium is known. Thus, the inverse problem arises — to determine the density of the medium $\rho(x, y, z)$ satisfying the relations (1)—(3), (10). The problem can be classified as a class of inverse problems with data given on the part of the boundary. The theoretical study of such statements in the case of receivers spaced out in space is very difficult (even for statements based on a second-order equation). Therefore we consider this problem only from the numerical point of view.

The inverse problem (1)—(3), (10) can be rewritten in operator form as follows:

$$A(\rho) = f, \qquad \rho(x, y, z) \to f_k(x, y, z, t), \quad k = 1, \dots, N. \qquad (11)$$

In [9] it was shown that in the 2D coefficient inverse problem for a hyperbolic equation, the operator A maps L_2 to L_2.

Let's reduce the inverse problem (1)—(3), (10) to minimizing the cost functional:

$$J(\rho) = ||A(\rho) - f||_{L_2}^2 =$$

$$= \sum_{k=1}^{N} \int_0^T \int_{\Omega_k} \left[p(x, y, z, t; \rho) - f_k(x, y, z, t) \right]^2 dxdydzdt \to \min_{\rho}. \qquad (12)$$

To minimize the functional (12) we apply the accelerated gradient method (heavy ball method):

$$\rho^{(n+1)} = \rho^{(n)} - \alpha J'(\rho^{(n)}) + \beta(\rho^{(n)} - \rho^{(n-1)}). \qquad (13)$$

Here $\alpha \in (0, ||A||^{-2})$ — descent parameter, $J'(\rho^{(n)})$ — gradient of the cost functional. Note that we have [5]:

$$J'(\rho) = 2 \left[A'(\rho) \right]^* (A(\rho) - f). \qquad (14)$$

Note that the heavy ball method can be rewritten as the conjugate gradient method in the case of minimizing the quadratic functional [59].

Here $[A'(\rho)]^*$ — the operator conjugate to the Frechet derivative of A. In [5], a theorem on the convergence of an iterative process was proved in the case when $\beta = 0$ in (13). If the following conditions holds true

(1) $\|A'(\rho)\| \le \mu < 1,$
(2) $\|A(\rho_1) - A(\rho_2) - A'(\rho_2)(\rho_1 - \rho_2)\| \le \eta\|A(\rho_1) - A(\rho_2)|, 0 < \eta < 1/2,$

then the Landweber iteration method is regularizing, and a strong convergence estimate is obtained. The fulfillment of the conditions of the theorem for a two-dimensional coefficient inverse problem for a hyperbolic equation was shown and an estimate of the strong convergence of the gradient method was obtained [9].

The initial guess for gradient descent is often chosen based on *a priori* information about the inverse problem solution. In the case of sufficiently accurate a priori information, and therefore a good initial guess, the number of iterations required to achieve a given accuracy can be significantly reduced [12, 46]. A modification of the gradient calculation method was presented in order to use as much data of the inverse problem as possible at each iteration [?]. In [?] it was presented a method of simultaneously calculating of the gradient and the conjugate problem, it reduces the amount of stored data in RAM memory by almost two times and reduces the calculation time by up to 25%. In [58], an algorithm based on a modification of the conjugate gradient method was proposed, and which takes into account rounding errors accumulated during calculations using the gradient descent method.

The gradient of the functional $J'(\rho)$ can be formally calculated by the formula [6, 31]:

$$J'(\rho)(x, y, z) =$$

$$= \int_0^T \left[-u\frac{\partial \Psi_1}{\partial t} - v\frac{\partial \Psi_2}{\partial t} - w\frac{\partial \Psi_3}{\partial t} + \frac{\Psi_4}{\rho(x, y, z)} \left(\frac{\partial u}{\partial x} + \frac{\partial v}{\partial y} + \frac{\partial w}{\partial z} \right) \right] dt. \quad (15)$$

Здесь Ψ_j, $j = 1, 2, 3$ — решение следующей сопряжённой задачи с неотражающими граничными условиями:

$$\frac{\partial \Psi_1}{\partial t} + \frac{1}{\rho} \frac{\partial \Psi_4}{\partial x} = 0; \tag{16}$$

$$\frac{\partial \Psi_2}{\partial t} + \frac{1}{\rho} \frac{\partial \Psi_4}{\partial y} = 0; \tag{17}$$

$$\frac{\partial \Psi_3}{\partial t} + \frac{1}{\rho} \frac{\partial \Psi_4}{\partial z} = 0; \tag{18}$$

$$\frac{\partial \Psi_4}{\partial t} + \rho c^2 \left(\frac{\partial \Psi_1}{\partial x} + \frac{\partial \Psi_2}{\partial y} + \frac{\partial \Psi_3}{\partial z} \right) =$$

$$= 2\rho c^2 \sum_{k=1}^{N} \theta_{\Omega_k}(x, y, z) \big[p(x, y, z, t) - f_k(x, y, z, t) \big]; \tag{19}$$

$$\Psi_i(x, y, z, T) = 0, \qquad i = 1, 2, 3, \tag{20}$$

with nonreflected boundary conditions.

Thus, each iteration of gradient descent implies the solution of the direct problem (1)–(3), using the current approximation ρ_n of the environment parameters, the subsequent solution of the conjugate problem (16)—(20) and simultaneous calculation of the gradient of the cost functional for the current time step using solutions of direct and conjugate problems (15). Since the conjugate problem (16)—(20) is a hyperbolic system of equations for its numerical solution, the Godunov scheme is used also.

4   Numerical results

The numerical calculations used synthetic data corresponding to a physical model, the acoustic parameters of which are close to the parameters of the human body [7, 8, 13].

The calculations used the following physical model: the object of study is placed in water, in which the source and receivers are located at the boundary. The cross section of the object is circles with a radius of 0.07 m, the distance from the center of the object to the sources and receivers in each slice is fixed and equal to 0.115 m. The acoustic parameters of the object (density and speed of sound in tissues) are selected in accordance with the parameters of human soft tissues ($\rho = 0.9$ kg/m^3, $c = 1.2$ km/s). Inclusions are also located inside the object, their shape, number and values of acoustic parameters are assumed to be unknown. Within the framework of the model, the values of the acoustic parameters of these inclusions were selected, exceeding the values in the 'healthy"fabrics. (the density was chosen in the range from $\rho = 1.1$kg/m^3 to $\rho = 1.3$ kg/m^3 in various inclusions, and the speed of sound varied from $c = 1.45$ km/s to $c = 1.6$ km/s). There was no information about inclusions in the initial approximation. The number of grid nodes was chosen to be equal for each of the spatial variables: $N_x = N_y = N_z = 120$. The dominant frequency of the probing signal during

the experiment was taken to be $\nu_0 = 20$ kHz. The descent parameter is $\alpha =$, $\beta = 0.8$.

For the initial experiments, the model shown in the figure 1 was chosen. It consists of two cylindrical inclusions inside the object. There are 16 receivers on each slice around the object. The cylindrical shape of the presented model was chosen in order to test the algorithm for solving 3D direct, conjugate and inverse problems, and it is not a necessary condition for the applicability of the algorithm. In further work, we plan to present the results of calculations for more complex geometry of inclusions, as well as the location of receivers.
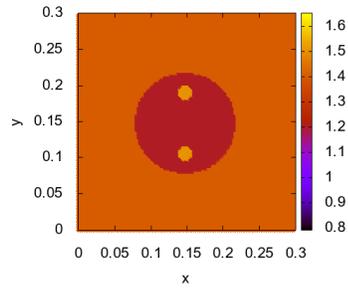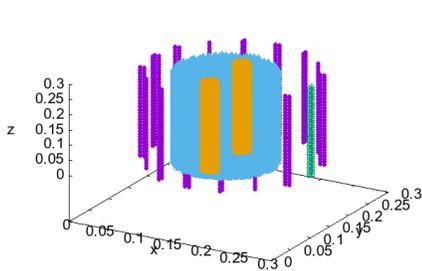

Distribution of the wave propagation velocity in a medium on an arbitrary slice along the z coordinate
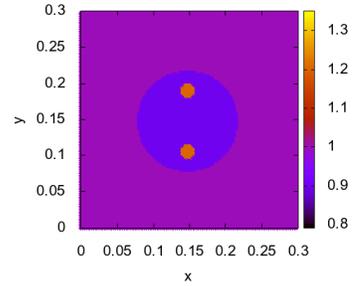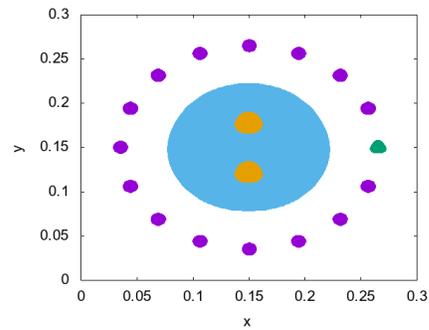
Distribution of the density of the medium on an arbitrary slice along the z coordinate

Рис. 1. The structure of the true model

3D model illustrating the locations of inclusions, sources, receivers and the object

A slice of the model at an arbitrary coordinate z

Рис. 2. The area of calculation is the cylinder. The sources are green, the receivers are purple, the object is blue, and the inclusions are yellow.
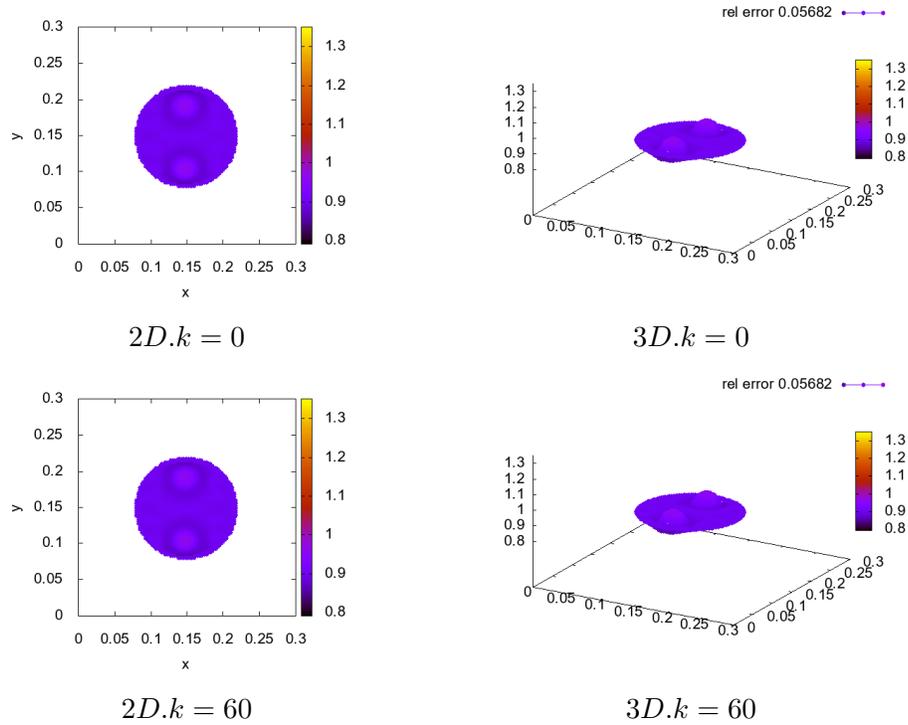
Рис. 3. Inverse problem solution after 70 iterations. The relative error is 0.0568

The results of solving the inverse problem by the gradient method after 500 iterations are shown in Figures 3—5. The parameter k corresponds to the coordinate of the variable z. Due to the cylindrical structure of our model, the values of the recoverable density of the medium must match on all slices, and this coincidence is shown in figures 3—5 both in three-dimensional form and in two-dimensional slices.

At each iteration of the algorithm, we calculate the relative error of the numerical solution:

$$RelError = \frac{||\rho_{exact} - \rho_{numeric}||}{||\rho_{exact}||}$$

The convergence of the iterative method in terms of functionality is illustrated by the figure 6. In this experiment, it can be observed that in the case of a fairly simple structure of the desired solution, the selected initial approximation turns out to be quite close to the solution, which demonstrates a decrease in the relative error during the numerical experiment (see Fig. 6).

To study the stability of the algorithm in question, we conducted an experiment with noisy data. A model with two cylindrical inclusions corresponding to the previous experiment was considered. Evenly distributed random noise was added to each of the receivers, corresponding to an error level of 15%.

$2D.k = 1$ $3D.k = 1$

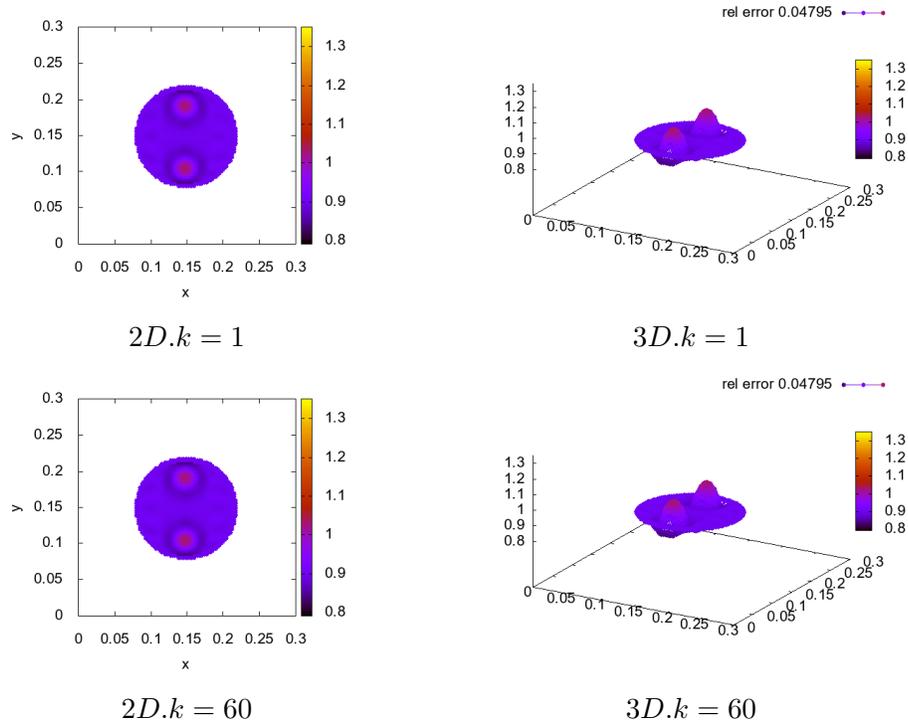$2D.k = 60$ $3D.k = 60$

Рис. 4. Inverse problem solution after 250 iterations. The relative error is 0.0479

The calculation results are shown in Figure 7. A characteristic difference of this experiment is the difference in the obtained slices. It is caused by the accumulation of errors associated with random noise in the receivers of the corresponding layers. As a result, the parameters are updated at each step of the iterative process in different ways on each slice, which indicates the correctness of the algorithms for solving three-dimensional direct and conjugate problems.

Note also that, although inclusions are clearly visible on each slice in the figure 7, various artifacts that do not correspond to the original model can also be observed in the above illustration. This is due to the fact that the incorrectness of the problem under consideration can lead to various features during the transition to optimization of the functional (12), for example, the presence of multiple local minima of the functional, resulting in a decrease in the discrepancy (12) may not mean convergence of the solution to the original one. In practice, there are various ways to overcome such effects, for example, the introduction of stabilizers in the formulation of the functional (12) or using the number of iterations as a regularization parameter (see, in particular, [?]). In addition, a priori information about the solution can be included in the initial approximation, which, in the case
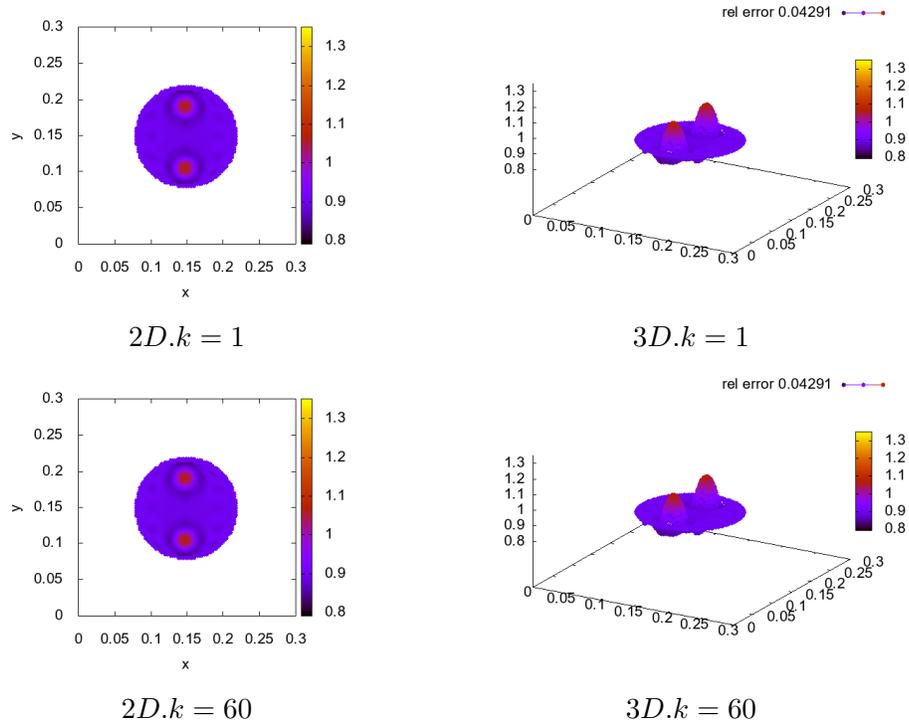
Рис. 5. The solution after 500 iterations. The relative error
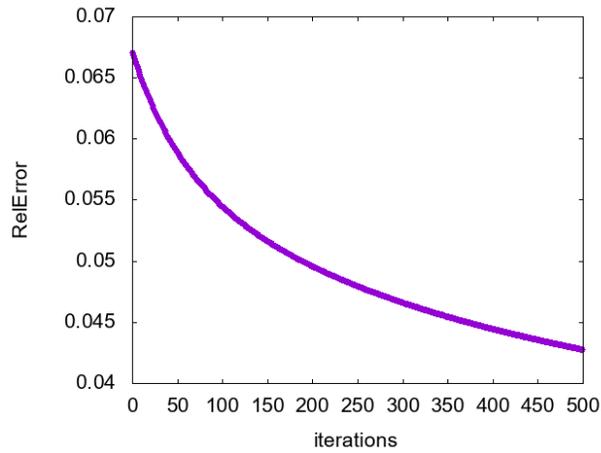is 0.0429

Рис. 6. Decreasing relative error

of reliable information, makes it possible to overcome the instability of the
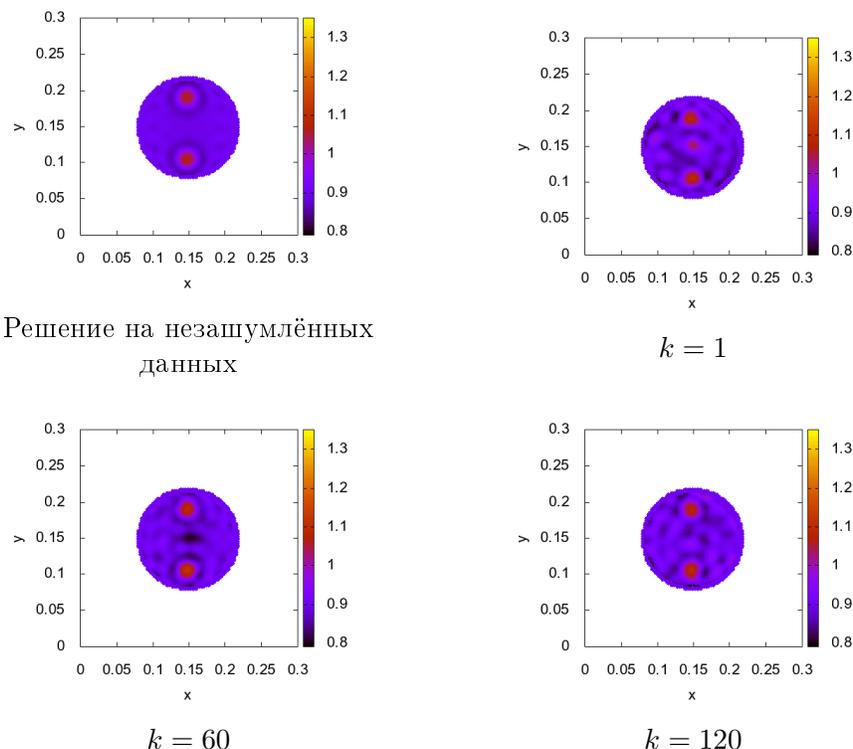problem to measurement errors.

Решение на незашумлённых
данных

$k = 1$

$k = 60$

$k = 120$

Рис. 7. Численные эксперименты с зашумлёнными данными

Заключение In this paper, we considered a 3D coefficient inverse problem for a hyperbolic system of first-order acoustic equations. The inverse problem is reduced to minimizing the cost functional by the gradient method. The gradient of the functional is calculated by solving a conjugate problem, which also has a hyperbolic type and for its solution we apply the same method as for a direct problem based on the Godunov type method. The advantages of the proposed approach, as noted in the introduction, is the possibility of direct and reverse modeling of acoustic tomography processes taking into account conservation laws. The results of the numerical experiment show the general applicability of the approach. However, the numerical complexity associated with the 3D of the formulation increases even more due to the iterative structure of the method and requires a large amount of computational resources to use the method even for relatively coarse grids. In future work, we will plan to consider ways to reduce the complexity of the method. The two main ways to do this are to reduce the computational cost of each iteration or reduce the total number of iterations. When considering the first method, various higher-order schemes can be considered. The total number of iterations required to obtain an acceptable accuracy of the solution can be reduced by using other methods (for example, data-based approaches

related to deep learning algorithms) to obtain a better initial approximation or by considering various schemes for minimizing the residual functional. In addition, it is planned to consider a more complex computational model in the future, when the geometry of the region and/or inclusions depends on the third dimension, use data with noise, and restore density and velocity simultaneously.

The authors are sincerely grateful to the anonymous reviewers for their valuable comments and advice, which significantly improved the content of the article.

References

[1] D.G. Northcott, *Ideal Theory*, Cambridge University Press, Cambridge, 1953.

[2] I.I. Ivanov, *Some properties of commutative algebras*, Siberian Electronic Mathematical Reports, **1** (2004), 142–143.

[3] A.V. Tetenov, M. Samuel, D.A. Vauilin, *On dendrites generated by polyhedral systems and their ramification points*, Trudy Inst. Mat. Mekh. UrO RAN, **23**:4 (2017), 281–291.

[4] Romanov, V.G.; Kabanikhin, S.I. *Inverse Problems for Maxwell's Equations*; VSP: Utrecht, The Netherlands, 1994.

[5] Hanke, M.; Neubauer, A.; Scherzer, O. A convergence analysis of the Landweber iteration for nonlinear ill-posed problems *Numer. Math.* **1995**, *72*, 21–37.

[6] He, S.; Kabanikhin, S.I. An optimization approach to a three-dimensional acoustic inverse problem in the time domain. *J. Math. Phys.* **1995**, *36*, 4028–4043.

[7] T. Douglas Mast. Empirical relationships between acoustic parameters in human soft tissues. Acoustics Research Letters. 2000. 1 (2). Pp. 37–42.

[8] Okawai H., Kobayashi K., Nitta S. An approach to acoustic properties of biological tissues using acoustic micrographs of attenuation constant and sound speed. Journal of Ultrasound in Medicine. 2001. 20: 891-907.

[9] Kabanikhin S.I., Scherzer O., Shishlenin M.A. Iteration methods for solving a two dimensional inverse problem for a hyperbolic equation. *J. Inverse Ill-Posed Probl.* **2003**, *11* (1) , 87–109.

[10] Романов В.Г., Глушкова Д.И. задача об определении двух коэффициентов гиперболического уравнения. Доклады Академии наук. 2003. Т. 390. No. 4. С. 452–456.

[11] D.I. Glushkova, V.G. Romanov. A stability estimate for a solution to the problem of determination of two coefficients of a hyperbolic equation. Siberian Mathematical Journal. 2003. Vol. 44, No. 2. P. 250–259.

[12] Kabanikhin, S.I.; Shishlenin, M.A. Quasi-solution in inverse coefficient problems. *J. Inverse Ill-Posed Probl.* **2008**, *16*, 705–713.

[13] Голубинский А.Н., Дворянкин С.В. К вопросу о параметризации результатов акустического зондирования тела человека при реализации контактно-разностного метода аудиоидентификации. Спецтехника и связь. 2011. No. 2. 38–43.

[14] Duric, N.; Littrup, P.; Li, C.; Roy, O.; Schmidt, S.; Janer, R.; Cheng, X.; Goll, J.; Rama, O.; Bey-Knight, L.; Greenway, W. Breast ultrasound tomography: Bridging the gap to clinical practice. *Proc. SPIE* **2012**, *8320*, 832000.

[15] Blokhin, A.M.; Trakhinin, Y.L. *Well-Posedness of Linear Hyperbolic Problems: Theory and Applications*; Nova Publishers, 2006.

[16] Marmot M G, Altman D G, Altman D G, Cameron D A, Dewar J A, Thompson S G and Wilcox M. The benefits and harms of breast cancer screening: an independent review Br. J. Cancer. 2013. 108 2205–2240.

[17] Wang K, Matthews T, Anis F, Li C, Duric N, Anastasio M. Waveform inversion with source encoding for breast sound speed reconstruction in ultrasound computed tomography IEEE Trans. Ultrason. Ferroelectr. Freq. Control. 2015. 62 475–493.

[18] Куликов И.М., Новиков Н.С., Шишленин М.А. Математическое моделирование распространения ультразвуковых волн в двумерной среде: прямая и обратная задача. Труды VI международной молодежной школы-конференции "Теория и численные методы решения обратных и некорректных задач". Сибирские электронные математические известия. 2015. Т. 12. С. 219—С.229.

[19] Burov, V.A.; Zotov, D.I.; Rumyantseva, O.D. Reconstruction of the sound velocity and absorption spatial distributions in soft biological tissue phantoms from experimental ultrasound tomography data. *Acoust. Phys.* **2015**, *61*, 231–248.

[20] Wiskin J W, Borup D T, Iuanow E, Klock J and Lenox M W 2017 3D nonlinear acoustic inverse scattering: algorithm and quantitative results IEEE Trans. Ultrason. Ferroelectr. Freq. Control 64 1161–1174.

[21] Hartmut Gemmeke, Torsten Hopp, Michael Zapf, Clemens Kaiser, Nicole V. Ruiter. 3D ultrasound computer tomography: Hardware setup, reconstruction methods and first clinical results. Nuclear Instruments and Methods in Physics Research Section A: Accelerators, Spectrometers, Detectors and Associated Equipment. 2017. Vol. 873. Pp. 59–65.

[22] Bernard S, Monteiller V, Komatitsch D, Lasaygues P 2017 Ultrasonic computed tomography based on full-waveform inversion for bone quantitative imaging Phys. Med. Biol. 62 7011–7035.

[23] P?rez-Liva M, Herraiz J L, Ud?as J M, Miller E, Cox B T, Treeby B E. Time domain reconstruction of sound speed and attenuation in ultrasound computed tomography using full wave inversion. J. Acoust. Soc. Am. 2017. 141, 1595–1604

[24] Opieli?ski K J, Pruchnicki P, Szymanowski P, Szepieniec W K, Szweda H, ?wi? E, J??wik M, Tenderenda M and Bu?kowski M. Multimodal ultrasound computer-assisted tomography: an approach to the recognition of breast lesions Comput. Med. Imaging Graph. 2018. 65 102–114.

[25] Malik B, Terry R, Wiskin J, Lenox M. Quantitative transmission ultrasound tomography: imaging and performance characteristics Med. Phys. 2018. 45 3063–3075.

[26] Guo R, Lu G, Qin B and Fei B. Ultrasound imaging technologies for breast cancer detection and management: a review Ultrasound Med. Biol. 2018. 44 37–70.

[27] Wiskin, J.; Malik, B.; Natesan, R.; Lenox, M. Quantitative assessment of breast density using transmission ultrasound tomography. *Med. Phys.* **2019**, *46*, 2610–2620.

[28] Sood R, Rositch A F, Shakoor D, Ambinder E, Pool K-L, Pollack E, Mollura D J, Mullen L A, Harvey S C. Ultrasound for breast cancer detection globally: a systematic review and meta-analysis J. Glob. Oncol. 2019. 5 1–17.

[29] Vourtsis A. Three-dimensional automated breast ultrasound: technical aspects and first results Diagn. Intervent. Radiol. 2019. 100 579–592

[30] Filatova, V.; Danilin, A.; Nosikova, V.; Pestov, L. Supercomputer Simulations of the Medical Ultrasound Tomography Problem. *Commun. Comput. Inf. Sci.* **2019**, *1063*, 297–308.

[31] Kabanikhin, S.I.; Klyuchinskiy, D.V.; Novikov, N.S.; Shishlenin, M.A. Numerics of acoustical 2D tomography based on the conservation laws. *J. Inverse Ill-Posed Probl.* **2020**, *28*, 287–297.

[32] Klyuchinskiy D.; Novikov N.; Shishlenin, M. A Modification of gradient descent method for solving coefficient inverse problem for acoustics equations. *Computation* **2020**, *8*, 73.

[33] Kozelkov A.S., Krutyakova O.L., Kurulin V.V., Strelets D.Yu., Shishlenin M.A. The accuracy of numerical simulation of the acoustic wave propagations in a liquid medium based on Navier-Stokes equations. Siberian Electronic Mathematical Reports. (2021). Vol. 18, No. 2. Pp. 1238–1250.

[34] Filatova V., Pestov L., Poddubskaya A. Detection of velocity and attenuation inclusions in the medical ultrasound tomography. Journal of Inverse and Ill-Posed Problems. 2021, 29(3), pp. 459–466

[35] Rumyantseva O.D., Shurup A.S., Zotov D.I. Possibilities for separation of scalar and vector characteristics of acoustic scatterer in tomographic polychromatic regime. Journal of Inverse and Ill-Posed Problems. 2021, 29(3), pp. 407–420.

[36] Klyuchinskiy, D.V., Novikov, N.S., Shishlenin, M.A. CPU-time and RAM memory optimization for solving dynamic inverse problems using gradient-based approach. Journal of Computational Physics. (2021) 439, No. 110374.

[37] Klyuchinskiy, D., Novikov, N., Shishlenin, M. Recovering density and speed of sound coefficients in the 2d hyperbolic system of acoustic equations of the first order by a finite number of observations. Mathematics. (2021). 9 (2), No. 199.

[38] Shishlenin M., Savchenko N., Novikov N., Klyuchinskiy D. Modeling of 2D Acoustic Radiation Patterns as a Control Problem. Mathematics, 2022, 10(7), 1116.

[39] Shurup A.S. Numerical comparison of iterative and functional-analytical algorithms for inverse acoustic scattering. Eurasian Journal of Mathematical and Computer Applications. 2022, 10(1), pp. 79–99.

[40] Li F, Villa U, Duric N, Anastasio MA. A forward model incorporating elevation-focused transducer properties for 3D full-waveform inversion in ultrasound computed tomography. IEEE Trans Ultrason Ferroelectr Freq Control. 2023. 70(10). 1339–1354.

[41] W. Zhao, Y. Fan, H. Wang, H. Gemmeke, Koen W.A. van Dongen, T. Hopp, J. Hesser. Simulation-to-real generalization for deep-learning-based refraction-corrected ultrasound tomography image reconstruction. Physics in Medicine and Biology. 2023. 68 035016

[42] L. Lozenski, H. Wang, B. Wohlberg, U. Villa, Y. Lin. Data driven methods for ultrasound computed tomography. Proc. SPIE 12463, Medical Imaging 2023: Physics of Medical Imaging, 124630Q.

[43] Shishlenin M., Kozelkov A., Novikov N. Nonlinear Medical Ultrasound Tomography: 3D Modeling of Sound Wave Propagation in Human Tissues. Mathematics. 2024, 12, 212.

[44] Романов В.Г. Лучевая постановка задачи акустической томографии. Доклады Российской академии наук. Математика, информатика, процессы управления. 2022. 505, No. 1. 50–55.

[45] Prikhodko, A., Shishlenin, M.A., Novikov, N.S., Klyuchinskiy, D.V. Encoder neural network in 2d acoustic tomography. Applied and Computational Mathematics. 2024, 23(1), 83–98.

[46] Кабанихин С.И., Шишленин М.А. Об использовании априорной информации в коэффициентных обратных задачах для гиперболических уравнений. Труды ИММ УрО РАН, 2012, т. 18, № 1, стр. 147–164.

[47] J. Wiskin, B. Malik, C. Ruoff, N. Pirshafiey, M. Lenox, J. Klock. Whole-Body Imaging Using Low Frequency Transmission Ultrasound, Academic Radiology. 2023. Vol. 30, Iss. 11. 2674–2685.

[48] Wiskin, J., Malik, B., Borup, D. et al. Full wave 3D inverse scattering transmission ultrasound tomography in the presence of high contrast. Sci Rep 10, 20166 (2020).

[49] Ozmen, N., Dapp, R., Zapf, M., Gemmeke, H., Ruiter, N. V., van Dongen, K. W. A. (2015). Comparing different ultrasound imaging methods for breast cancer detection. IEEE Transactions on Ultrasonics, Ferroelectrics, and Frequency Control, 62(4), 637–646.

[50] Годунов С.К., Забродин А.В., Иванов М.Я., Крайко А.Н., Прокопов Г.П. Численное решение многомерных задач газовой динамики. Москва, Наука. 1976.

[51] Matthews T P, Wang K, Li C, Duric N and Anastasio M A. Regularized dual averaging image reconstruction for full-wave ultrasound computed tomography IEEE Trans. Ultrason. Ferroelectr. Freq. Control. 2017. 64 811–825.

[52] Beilina L., Cristofol M., Li S., Yamamoto M. Lipschitz stability for an inverse hyperbolic problem of determining two coefficients by a finite number of observations. Inverse Problems. 2017, 34, 015001.

[53] L. Beilina, M. Cristofol, Sh. Li. (2018) Determining the conductivity for a nonautonomous hyperbolic operator in a cylindrical domain. Mathematical Methods in the Applied Sciences 41:5, pages 2012-2030.

[54] Michael V. Klibanov, Alexandre Timonov. A comparative study of two globally convergent numerical methods for acoustic tomography. Communications on Analysis and Computation, 2023, 1(1): 12-31.

[55] T.G. Muir, E.L. Carstensen. Prediction of nonlinear acoustic effects at biomedical frequencies and intensities. Ultrasound in Medicine and Biology. 1980. Vol. 6, Issue 4. Pages 345–357.

[56] B. Kaltenbacher. Mathematics of nonlinear acoustics. Evolution Equations and Control Theory. 2015. 4(4). 447–491.

[57] Б.Т. Поляк. О некоторых способах ускорения сходимости итерационных методов. Ж. вычисл. матем. и матем. физ., 4:5 (1964), 791–803.

[58] Lukyanenko, D.; Shinkarev, V.; Yagola, A. Accounting for round-off errors when using gradient minimization methods. Algorithms 2022, 15, 324.

[59] Alexandre d'Aspremont, Damien Scieur, Adrien Taylor. Acceleration Methods. Foundations and Trends® in Optimization. 2021. Vol. 5: No. 1–2, pp 1–245.

[60] Shishlenin M.A., Savchenko N.A., Novikov N.S., Klyuchinskiy D.V. On the reconstruction of the absorption coefficient for the 2d acoustic system. Siberian Electronic Mathematical Reports. 2023, 20(2), 1474–1489.

[61] Kabanikhin S.I., Shishlenin M.A. Theory and numerical methods for solving inverse and ill-posedproblems. Journal of Inverse and Ill-Posed Problems. 2019. 27(3), Pp. 453–456.